CHAPTER 5

ANTIBACTERIAL AND DNA DEGRADATION POTENTIAL OF Ag-NPs

A part of this chapter has been published in the following article:

1. D. K. Manna, A. K. Mandal, I. K. Sen, P. K. Maji, S. Chakraborti, R. Chakraborty, S. S. Islam. International Journal of Biological Macromolecules; 80, 455–459, 2015.

5.1. Introduction and review of earlier works

Bacteria have the potential to develop resistance against commercially available antibiotics. If they are competent to resist at least two or more antibiotic, they are generally termed as multiple antibiotic resistant (MAR) bacteria or superbug [253]. *Escherichia coli* (*E. coli*) is a common pathogen linked with community-associated as well as nosocomial infections. In the last few decades, the resistant *E. coli* strains towards broad-spectrum antimicrobials were reported [254-255]. Resistance of pathogenic bacteria towards multiple antimicrobial agents has become a major threat to public health as there are no effective antimicrobial agents available to treat these infections [256-257]. This alarming threat caused by infection due to MAR bacteria opened up a way to synthesize new class of antimicrobials. Recently, metal nanoparticles have gained importance in optical, electronic, catalytic and magnetic field for their unusual properties and various applications [257-259]. A common method for the preparation of metal nanoparticles involves the treatment of metal salt with a chemical reducing agent such as citrate salt, borohydride, formaldehyde, and solvent like N, N-dimethyl formamide (DMF) and ethylene glycol [260-262]. All these chemicals cause potential environmental and biological toxicity. Hence, there is an urgent need of green method for synthesis of various nanoparticles using environmental caring solvent and nontoxic renewable materials. Biomolecules and living organisms are useful sources for the synthesis of these nanomaterials where they act both as reducing and stabilizing agents [263-265]. It was reported earlier that AgNPs can be synthesized using β-D-glucose as reducing and starch as stabilizing agent [266]. In a separate study synthesis and stabilization of AgNPS were performed using chitosan and spent mushroom substrate [267-268]. Recently, the synthesis of AuNPs using (1→3)-, (1→6)-α, β-D-glucan of an edible mushroom [269] and a gum polysaccharide of *Cochlospermum religiosum* (katira gum) [270] have been reported. The antibacterial activity of the silver nanoparticles was established to prevent bacterial colonization on catheters [271] and vascular grafts [272]. In the present work silver nanoparticles were prepared using the hetero polysaccharide isolated from an aqueous extract of an edible mushroom, *Lentinus squarrosulus* (Mont.) Singer [273]. The efficacy of AgNPs-PS conjugates was studied against a MAR bacterium, *E. coli* MREC33. Hemolytic activity of AgNPs-PS conjugates was also studied in order to

find out the degree of toxicity toward human RBCs. Further, the synergistic antibacterial effect of AgNPs-PS conjugates at LD_{50} dosage in combination with each of the antibiotics ampicillin, azithromycin, kanamycin, and netilmicin against the MAR bacterium *E. coli* MREC33 was investigated and the results are reported herein.

5.2. Present work

5.2.1. Synthesis and characterization of AgNPs

A hetero polysaccharide (**Figure 5.1**) was isolated from hot water extract of fresh fruit bodies of an edible mushroom, *Lentinus squarrosulus* (Mont.) Singer. The structure of the polysaccharide was confirmed using chemical and NMR analysis [273] and reported as:

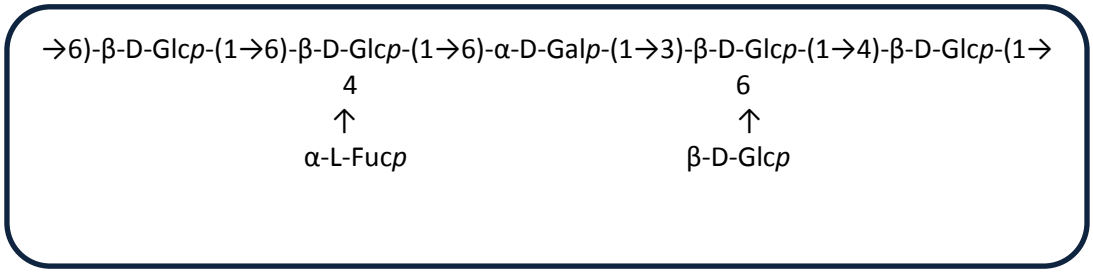

Figure 5.1: Structure of hetero polysaccharide isolated from hot water extract of *Lentinus squarrosulus* (Mont.) Singer.

AgNPs–PS conjugates were prepared by chemical reduction of of 2 mM $AgNO_3$ solution with 0.025%, 0.05% and 0.1% (w/v) solution of polysaccharide in water. An absorption peak started to appear at 404 nm after heating 65^0C for 7 h which is a typical surface plasmon resonance (SPR) band for AgNPs as reported by Vigneshwaranet al. [268]. Absorption intensity increases with time which is due to the reduction of silver ions to elemental silver. Maximum intensity of the absorption band occurred after 21 h of the reaction and there after no significant change was observed indicating complete reduction of silver ions (**Figure 5.2**).

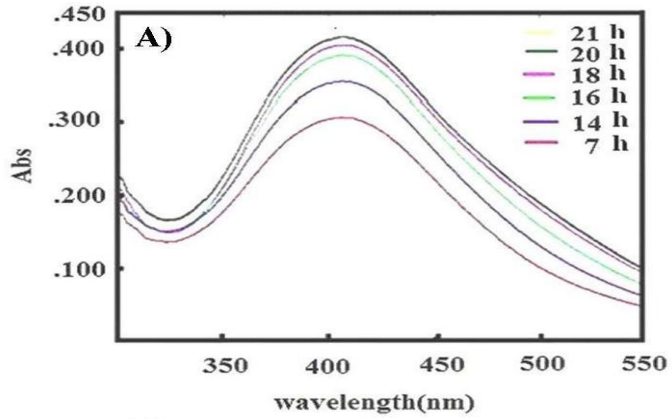

Figure 5.2: UV-vis spectra of AgNPs–PS with 0.05% (w/v) of PS at different time intervals. The peak at around 404 nm corresponds to the SPR of AgNPs.

The NPs prepared with 0.025% and 0.1% (w/v) PS shows maximum absorption peak at 423 nm and 449 nm, respectively (**Figure 5.3a** and **Figure 5.3b**). The red-shift of SPR bands indicates that the particle size were larger compared to the NPs prepared with 0.05% PS [274]. Thus, throughout the whole study AgNPs prepared with 0.05% (w/v) of PS was used.

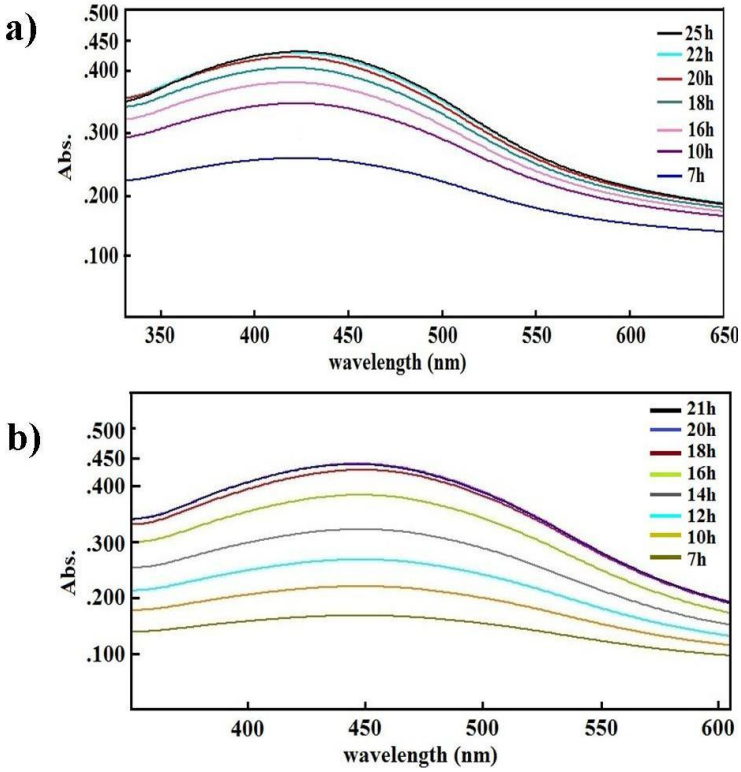

Figure 5.3: UV-vis spectra of AgNPs–PS at different time intervals a) with 0.025% (w/v) of PS. The SPR peak at around 423 nm b) with 0.025% (w/v) of PS. The SPR peak at around 449 nm.

HR-TEM image (**Figure 5.4a**) showed that the NPs are mostly spherical and well separated with average size of 2.78 ± 1nm as analyzed from the size distribution histogram (**Figure 5.4b**) of the nanoparticles.

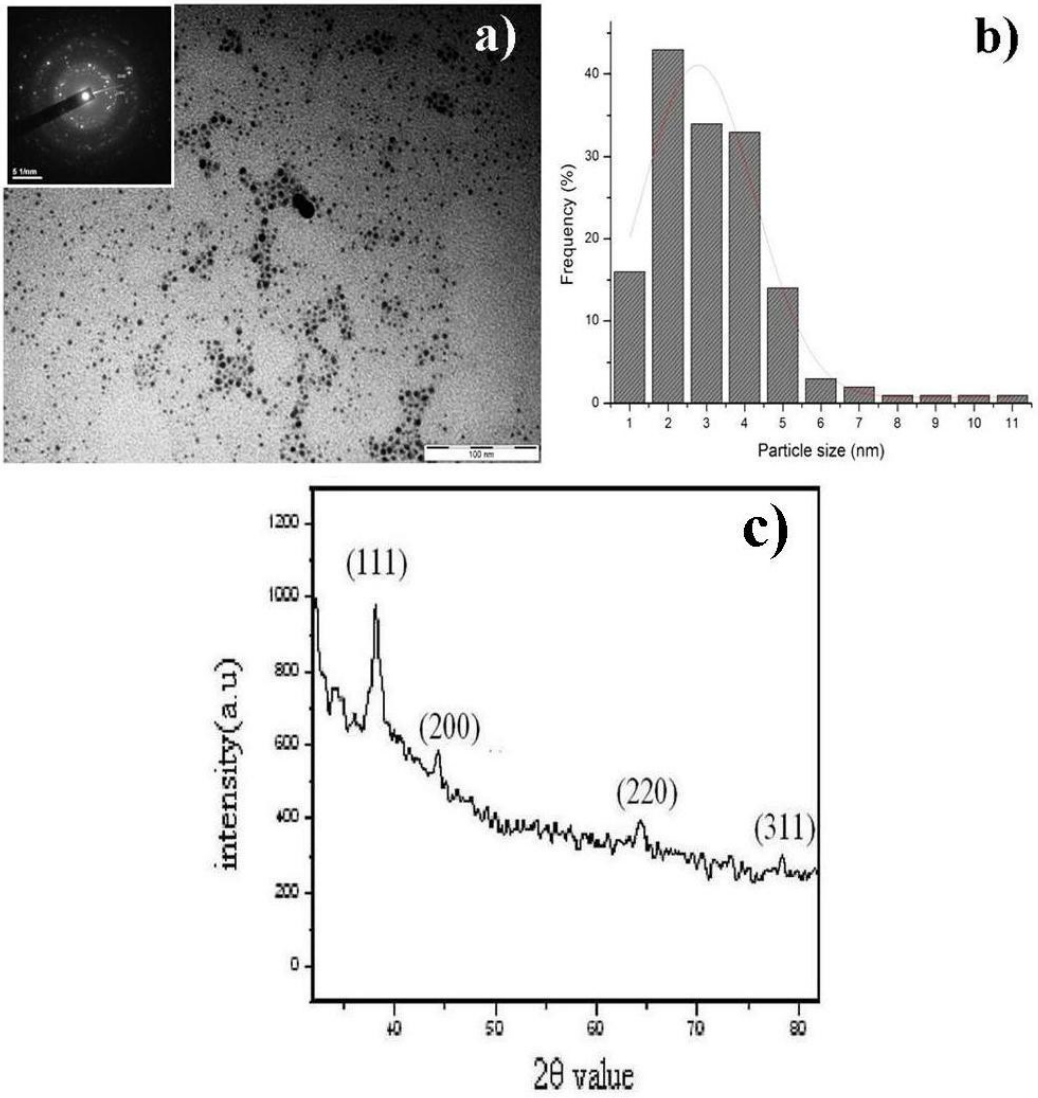

Figure 5.4: (a) TEM images and the corresponding selected area electron diffraction (SAED) patterns (inset) of AgNPs-PS. (b) Particle size distribution histogram. (c) XRD patterns of freeze dried AgNPs- glucan conjugates, all the peaks could be indexed to fcc lattice of silver.

The selected area diffraction pattern (SAED), **Figure 5.4a** inset, confirmed the 'fcc' crystalline structure of Ag NPs–PS conjugates and presence of four planes (1 1 1), (2 0 0), (2 2 0), and (3 1 1). The crystalline nature of Ag NPs was further confirmed by the X-ray diffraction analysis (**Figure 5.4c**).

The XRD diffraction peaks at 38.11◦, 44.20◦, 64.42◦, and 77.46◦corresponded to the (1 1 1), (2 0 0), (2 2 0), and (3 1 1) planes respectively of face-centered cubic (fcc) silver. This result was also confirmed by SAED. It was observed that intensity of the (1 1 1) plane is higher than the other planes.

5.2.2. Antibacterial activity of AgNPs-PS conjugates

The antibacterial activity was studied with mono dispersed suspensions of AgNPs-PS conjugates at different concentrations in deionized water on MAR bacterium, *Escherichia coli* MREC33. The negative control (without NPs) showed the normal growth profile of MREC33. The bacterial growth rate (in comparison with the control) was found slower with increasing concentrations (5, 10, 20, and 40 µg/ml) of Ag NPs–PS conjugates. The LD_{50} (50% inhibition in bacterial growth in the test sample) was observed 5 µg/mL while minimum inhibitory concentration (MIC) for NPs was found 40 µg/mL (**Figure 5.5**).

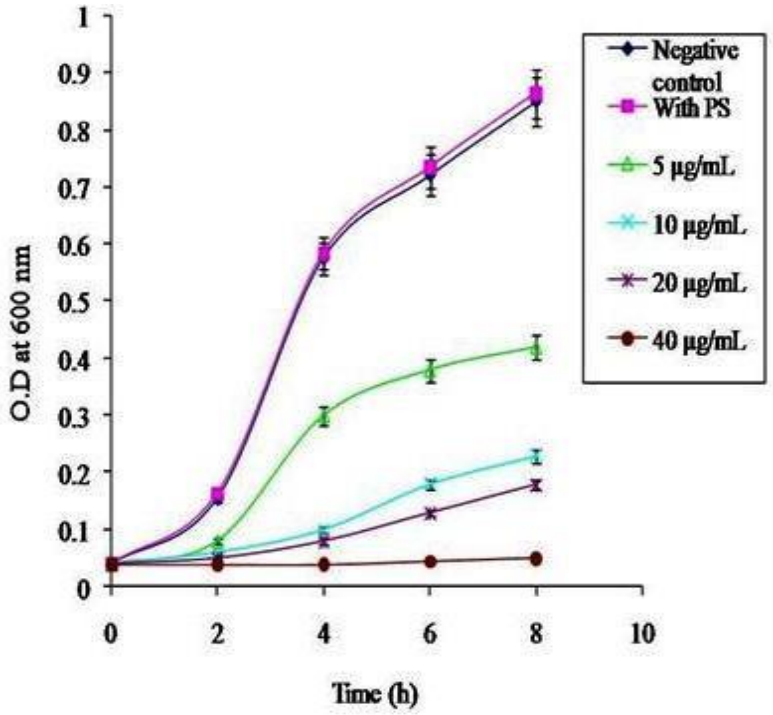

Figure 5.5: Efect of varying concentration of Ag NPs–PS conjugates on the growth of Escherichia coli strain MREC33 in MH broth.

5.2.3. DNA degradation study

DNA damage of log phase *E. coli* MREC33 cells by AgNPs-PS was determined by means of FACS analysis. DAPI preferentially bind to A-T rich sites of ds-DNA and binding causes almost 20-fold increment in fluorescence intensity [274-276]. Similar type of enhancement in fluorescence intensity was observed when MREC33 cells were treated with DAPI only (control). Interestingly, when the same bacterial cells were exposed to AgNPs-PS conjugates along with DAPI, a decrease in fluorescence intensity was observed compared to that of control (**Figure 5.6a and 5.6b**). This may be possible due to detachments of bound DAPI from A-T rich sites of the ds-DNA. It was reported earlier that ROS reacts with DNA by addition to double bonds of nucleo bases and abstract H-atom from the methyl group of thymine [277-278] causing damage at A-T rich sites, enhancing free DAPI concentration with concomitant decrease in fluorescence intensity. Hence, the above experiments prove AgNPs-PS conjugates have induced generation of intercellular ROS which caused DNA damage within the live cells. Moreover, *E. coli* MREC33 cells after treatment with AgNPs-PS conjugates have shown increase in side scattering (SSC) intensity compared to that of control supporting our claim of internalization of AgNPs-PS conjugates inside the bacterial cells (**Figure 5.6c and 5.6d**).

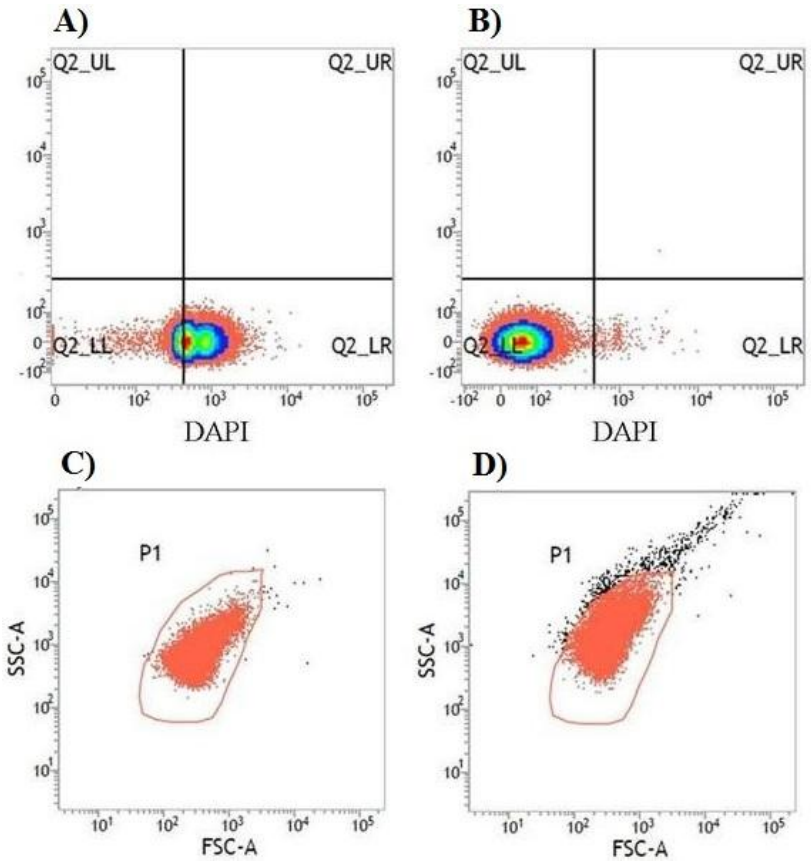

Figure 5.6. DNA degradation using FACS analysis of *E. coli* MREC33 cells (A) DAPI treated control cells; (B) cells treated with DAPI and 40 µg/mL AgNPs–PS conjugates. Side scattering analysis of: (C) DAPI treated control cell; and (D) AgNP–PS and DAPI treated MREC33 cell using FACS.

5.2.4. Hemolysis assay

As nanoparticles, after being administered, are translocated rapidly via blood into different organs [279], the toxicity of Ag NPs was evaluated with reference to percent hemolysis. The hemolytic activity of 1.017 % was observed at 5 µg/ml Ag NPs-PS conjugates (Figure 5.7). The result suggests that Ag NPs-PS conjugates at LD_{50} concentration in combination with conventional antibiotics may be considered as less hazardous for intravascular drug delivery. In an earlier study, toxic effect of starch capped Ag NPs was found to be lesser than polyvinyl alcohol (PVA) capped Ag NPs on red blood cells (RBCs) [280]. Materials with a hemolysis ratio less than 5% were regarded as hemo compatible [231]. Thus, a dose of 5 µg/ml (LD_{50}) of AgNPs-PS conjugates was found to be compatible with RBCs.

Figure 5.7. Hemolysis study of human RBCs treated with LD_{50} concentration of AgNPs–PS conjugates. RBCs suspended in water used as positive control and in PBS as negative control.

5.2.5. Synergistic effects with antibiotics

It was observed that LD_{50} dosage (5 µg/ml) of AgNPs glucan conjugates inhibited 50% of the bacterial growth while any of the four antibiotics ampicillin (50 µg/ml), azithromycin (10 µg/ml), kanamycin (10 µg/ml) and netilimicin (20 µg/ml) did not affect the growth of *E. coli* MREC33 strain. But when each of the antibiotics combined individually with 5 µg/ml of AgNPs-PS conjugates, almost 100% inhibition of bacterial growth was achieved. This phenomenon suggests additive or synergistic bactericidal effect on multiple antibiotic resistant *E. coli* MREC33.

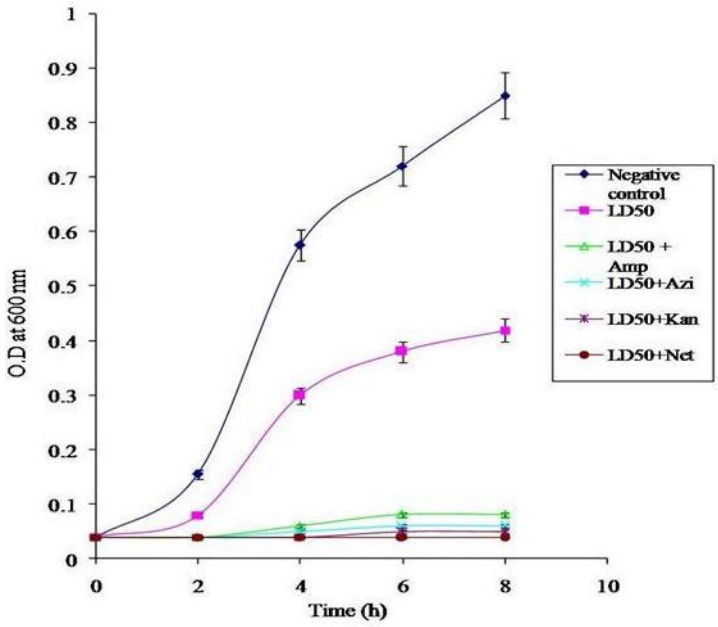

Figure 5.8. Synergistic antibacterial effects of the Ag NPs–PS conjugate at 5 µg/ml in combination with (a) ampicillin, (b) azithromycin, (c) kanamycinand (d) netilmicin.

5.2.6. Conclusion

The present study demonstrated a simple and effective green route for synthesis of silver nanoparticles using hetero polysaccharide obtained from edible mushroom, *L. squarrosulus (Mont.) Singer*. As, polysaccharide fulfilled the dual purpose of reducing as well as stabilizing agent for the preparation of NPs, no external toxic reducing agent were needed. The average size of the nanoparticles was found to be 2.78 ± 1.47 nm. The bactericidal property of the synthesized AgNPs–PS conjugates was studied against multiple antibiotic resistant (MAR) bacterium, E. coli MREC33. DNA fragmentation study using FACS enabled to understand the mode of action of NPs. AgNPs–PS conjugates were also found to be compatible with human RBCs at its LD_{50} dosage. Finally, synergistic antibacterial effect was noted with the hemocompatible dosage of AgNPs–PS conjugates when used in combination with various antibiotics.